ISSN 0023-1584, Kinetics and Catalysis, 2011, Vol. 52, No. 4, pp. 605–619. © Pleiades Publishing, Ltd., 2011.
Original Russian Text © A.M. Volodin, S.E. Malykhin, G.M. Zhidomirov, 2011, published in Kinetika i Kataliz, 2011, Vol. 52, No. 4, pp. 615–629.

Dedicated to the 80th birthday of Academician V.B. Kazanskii

O^- Radical Anions on Oxide Catalysts: Formation, Properties, and Reactions

A. M. Volodin[a, *], S. E. Malykhin[a], and G. M. Zhidomirov[a, b]

[a] *Boreskov Institute of Catalysis, Siberian Branch, Russian Academy of Sciences, Novosibirsk, 630090 Russia*
[b] *Zelinsky Institute of Organic Chemistry, Russian Academy of Sciences, Moscow, 119991 Russia*
**e-mail: volodin@catalysis.ru*

Received December 16, 2010

Abstract—A systematic in situ EPR study of processes yielding O^- radical anions on the surface of oxide dielectrics (MgO, CaO), semiconductors (ZnO, TiO_2), supported systems (V/SiO_2), and zeolite FeZSM-5 is reported. Methodological approaches to the study of O^- radical anions are considered for the cases in which these species are directly undetectable by EPR. Particular attention is focused on the development of methods of investigation of so-called α-oxygen on the FeZSM-5 surface, which is an O^- radical anion stabilized on the paramagnetic ion Fe^{3+}. The reactions involving α-oxygen and the analogous reactions known for O^- radical anions stabilized on the oxide surface are demonstrated to occur in similar ways. The photostimulated formation of spatially separated electron and hole centers on the surface of oxide systems is most likely due not to charge separation, but to the spatial separation of the radicals resulting from the homolytic photodissociation of chemisorbed water. A scheme is suggested for this process on the partially hydroxylated MgO surface.

DOI: 10.1134/S0023158411040173

Radicals of adsorbed oxygen as possible intermediates in oxidation catalysis and photocatalysis on oxide systems have been attracting researchers' attention for more than half-century [1–6]. EPR spectroscopic studies have made a considerable contribution to the development of this area. In a number of cases, this method has made it possible to directly observe O^-, O_2^-, and O_3^- radical anions stabilized on the surface of oxide catalysts and to investigate reactions of these species. The most important results obtained in this field have been reported in detail in original works and reviews [7–12].

At the same time, it is obvious that long-lived anion radicals directly detectable by EPR do not cover all possible species involved as intermediates in catalytic reactions. There have been only a few reports on process involving these radicals on the surface of oxide semiconductors, which proved to be efficient photocatalysts.

The formation, stabilization, and reactivity of each of the above radical anions have their own specific features. A particularly large number of formation routes are known for the molecular radical anion O_2^- on oxide surfaces [4, 9, 13–16]. This radical anion is a convenient spin probe for studying of active sites of oxide catalysts. However, its participation in high-temperature oxidation catalysis seems rather unlikely. As judged from the literature, the molecular radical anion O_2^- is likely involved in liquid-phase oxidations using H_2O_2 as the oxidizer. This species is extremely unstable on the sulfated ZrO_2 surface, which may be due to its protonation on this strong acid catalyst [15]. However, reactions involving O_2^- are beyond the scope of this work. In this review, we will limit out consideration to the atomic radical anion O^-, a possible key intermediate in a variety of oxidation catalysis and photocatalysis processes [1–6].

The radical anion O^-, with an electron spin of $S = 1/2$, can be directly detected by EPR spectroscopy only provided that the following specific conditions are satisfied: (1) The radical anion should be fairly stable, so that its lifetime is sufficiently long for recording an EPR spectrum. (2) The nearest paramagnetic neighbor of O^- should be fairly far away, so that there are no exchange-coupled complexes (which are possible at $d < 0.5$ nm) and no considerable mutual broadening of EPR lines due to dipole–dipole interactions. Use of the formula $\Delta H \sim 4\mu_e/r^3$ [17] (where ΔH is the contribution from the dipole–dipole interactions to the line width, μ_e is the magnetic moment of an electron, and r is the average distance between the nearest paramagnetic centers) for randomly oriented paramagnetic centers leads to a characteristic radical anion–para-

magnetic neighbor distance of at least 2 nm for a typical experimental line width of $H \sim 1-2$ G. (3) The relaxation properties of the radical anion should be suitable for recording its EPR spectrum under conventional conditions (77–373 K, microwave power of $10^{-2}-10^{2}$ mW). This implies the elimination of the degeneracy of the p_x and p_y orbitals of O^- via their interaction with the crystal field of the cation stabilizing O^- [7, 8]. (4) The O^- stabilization center should be diamagnetic. This means that the Me^{n+} cation in the $[Me^{n+}...O^-]$ complex should not possess intrinsic paramagnetism. This situation is fairly typical for the cations Zn^{2+}, Ti^{4+}, Mg^{2+}, Ca^{2+}, V^{5+}, Mo^{6+}, etc. Obviously, this situation will not take place for the stabilization of the radical anion on paramagnetic ions (Fe^{2+}, Fe^{3+}, Mn^{2+}, Cu^{2+}, etc.).

Simultaneous fulfillment of the above four conditions is a rather stringent requirement. It is far from being always satisfied when O^- forms on the oxide surface. Therefore, in many cases O^- can appear and exist on the catalyst surface without being directly detectable by EPR spectroscopy. This situation is poorly reflected in the present-day literature. Discussion and analysis of this situation are among the purposes of this review.

Here, we will report the results of an in situ EPR investigation of the formation mechanism and reactions of the radical anion O^- on the surface of a supported catalyst (V/SiO_2), dielectric oxides (MgO, CaO), oxide semiconductors (ZnO, TiO_2), and zeolite FeZSM-5. Special attention will be focused on the cases in which the radical anion is, for some reason, directly undetectable by EPR and special-purpose techniques should be used to make it observable by EPR and amenable to investigation.

The experimental procedure, catalysts, and their conditioning have already been described in detail [4, 10–13]. In all cases, unless otherwise stated, the samples were subjected to prolonged oxygen–vacuum treatment at 773 K, which was carried out for removing adsorbed water, CO_2, and "biographical" organic impurities.

FORMATION AND REACTIONS OF O^- RADICAL ANIONS ON THE SURFACE OF OXIDE CATALYSTS

Photostimulated and Thermal Processes on V/SiO_2 Catalysts

A typical example of a short-lived state of the radical anion O^- coordinated to a paramagnetic cation (two of the above conditions—(1) and (2)—are not satisfied) is the charge-transfer state $[V^{4+}...O^-]^*$, which results from the photoexcitation of vanadyl complexes in V/SiO_2 catalysts:

$$\left[V^{5+}...O^{2-}\right] \underset{\longleftarrow}{\overset{h\nu}{\longrightarrow}} \left[V^{4+}...O^{-}\right]^*. \qquad \text{(I)}$$

Such states are unobservable by EPR, but they are reliably identifiable by luminescent methods [18–21]. Their lifetimes are at the millisecond level and are sufficiently long for their O^- radical anions to react with molecules from the gas phase. It is these intermediates that are responsible for the photoreduction of vanadium complexes in V/SiO_2 [18, 19, 21–23]:

$$\left[V^{4+}...O^{-}\right]^* + RH \rightarrow \left[V^{4+}...OH^{-}\right] + R^{\bullet}. \qquad \text{(II)}$$

The tetravalent vanadium complex $[V^{4+}...OH^-]$ resulting from this photoreduction is stable at room temperature and is reliably detectable by EPR [21, 23]. Similar processes are known for many supported catalysts [19, 24] and low-coordinated structures on oxide surfaces [25].

Note that V/SiO_2 is among the few systems in which stabilized O^- radical anions result from the reoxidation of the reduced catalyst due to the adsorption of N_2O and O_2 molecules [7, 8, 26–29]. A remarkable specific feature of these processes is that, up to 673 K, N_2O oxidizes only its "own" sites and does not react with O_2 adsorption sites [28]. Let us consider these processes in greater detail. The mechanism of O^- formation via N_2O adsorption on the surface of reduced (or photoreduced) oxide catalysts, which is well known from the literature, is fairly simple and is commonly associated with the adsorption of an N_2O molecule on an electron-excessive surface site [e]:

$$[e] + N_2O \rightarrow N_2O^- \rightarrow N_2 + O^-. \qquad \text{(III)}$$

In the case of the V/SiO_2 system, the role of this reduction-generated site is played by the V^{4+} ion:

$$\begin{aligned}\left[V^{4+}\right] + N_2O &\rightarrow \left[V^{5+}\ldots N_2O^-\right] \\ &\rightarrow \left[V^{5+}\ldots O^-\right] + N_2.\end{aligned} \qquad \text{(IIIa)}$$

The mechanism of O^- formation via oxygen adsorption is not so obvious. It is generally assumed in the literature that the reoxidation of reduced oxides involves the following sequence of reactions of adsorbed oxygen molecules:

$$\begin{aligned}O_2 \Leftrightarrow (O_2)_s &\xrightarrow{+e} \left(O_2^-\right)_s \\ \xrightarrow{+e}\ 2\left(O^-\right)_s &\xrightarrow{+2e} 2\left(O^{2-}\right)_s \rightarrow 2\left(O^{2-}\right)_{latt}.\end{aligned} \qquad \text{(IV)}$$

This scheme was suggested long ago and, since then, has been widely discussed [1, 2, 5, 27]. No significant changes have been made to this scheme to date [6]. Nevertheless, according to our knowledge, there is still no convincing evidence that the reoxidation processes take place via this scheme. Particularly doubtful is the step

$$\left(O_2^-\right)_s + e \rightarrow 2\left(O^-\right)_s, \qquad \text{(V)}$$

in the consecutive conversions of the molecular oxygen radical anion into atomic species in the reoxidation of reduced oxide systems. Conversely, the totality

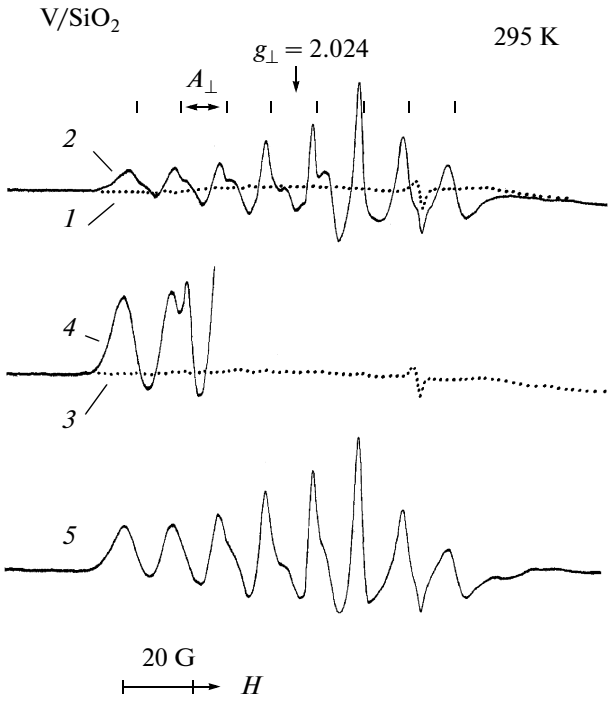

Fig. 1. EPR spectra of a V/SiO_2 catalyst sample successively subjected to the following treatments: (*1*) reduction with H_2 (3 Torr) at 760 K for 4 h, (*2*) N_2O adsorption at 295 K, (*3*) additional heating in N_2O at 670 K followed by pumping at this temperature and N_2O adsorption at 295 K, (*4*) pumping at 295 K and O_2 adsorption (0.15 Torr) at the same temperature, and (*5*) pumping at 470 K. The spectra were recorded at 295 K.

of presently available relevant EPR data indicates that, after the formation of stabilized $\left(O_2^-\right)_s$ and $(O^-)_s$ radical anions separated by sufficiently long distance, they participate independently in subsequent chemical reactions [4, 10–12].

Figure 1 displays EPR spectra typical of oxygen radical anions appearing during the reoxidation of a partially reduced V/SiO_2 catalyst by N_2O and O_2 molecules. Note that, in all cases, the radical yield in the reoxidation of the reduced catalyst does not exceed 1–5% of the total amount of oxygen spent for reoxidation. At the same time, the entire oxygen necessary for the reoxidation is chemisorbed even at room temperature [28]. It can readily be seen that, up to 670 K, N_2O molecules can oxidize only their "own" sites (Fig. 1, curves *2*, *3*). The sites responsible for the formation of radical anions upon oxygen adsorption are not oxidized under these conditions. Subsequent O_2 adsorption yields O^- and O_2^- radical anions (Fig. 1, curve *4*). Short-term pumping of this sample at 470 K eliminates the line due to O_2^- (Fig. 1, curve *5*) owing to the shift of the equilibrium

$$O_2^- \rightleftarrows e + O_2 \qquad \text{(VI)}$$

to the right. The radical anion O^- is fairly stable under these conditions and is observable by EPR spectroscopy (Fig. 1, curve *5*).

Our detailed analysis of the formation and disappearance conditions for the adsorbed oxygen radicals generated during the reoxidation of the partially reduced V_2O_5/SiO_2 catalyst [28] demonstrated that the most likely mechanism of the formation of the oxygen radical anions stabilized on the surface of this catalyst is the formation of $[V^{4+} \ldots O^-]^*$ charge-transfer complexes via the reoxidation of the vanadium catalyst by oxygen followed by the stabilization of the spatially separated radical anions $(O_2^-)_s$ and $(O^-)_s$:

$$\left[V^{4+}\ldots O^-\right]^* \xrightarrow{O_2} \left(O^-\right)_s + \left(O_2^-\right)_s. \qquad \text{(VII)}$$

Thus, the excited triplet states of the $[V^{4+}\ldots O^-]^*$ complexes can result both from photostimulated reactions and from ordinary redox reactions and can be responsible for the formation of oxygen radical anions. Note that the possible participation of these charge-transfer complexes in oxidation catalysis was discussed in a number of works [6, 20, 30].

Photostimulated Formation of O⁻ Radical Anions on the Surface of Oxide Semiconductors and Dielectrics

Nearly all of the known ways of generating O^- radical anions on the surface of oxide systems somehow involve irradiation. These species are directly generated as holes by irradiation with light in the absorption

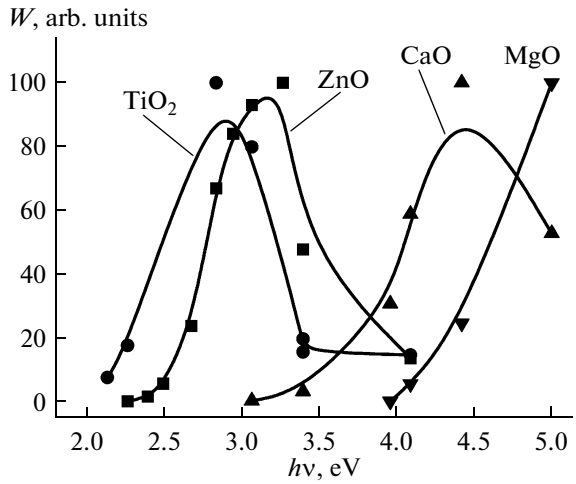

Fig. 2. Spectral dependences of the initial rate of the photostimulated formation of oxygen radical species on the surface of TiO_2 [3, 35], ZnO [4], MgO [10, 12], and CaO [11, 12].

region of surface $[Me^{n+}... O^{2-}]_{LC}$ complexes containing a low-coordinated (LC) ion [3, 4, 10–12, 31] or are produced via preliminary generation of electron centers [e] by UV irradiation in a hydrogen medium followed by N_2O adsorption [32–34]. All of these processes involve the initial nonparamagnetic surface complex responsible for the primary absorption of light quanta. Therefore, the spectral characteristics of the photostimulated processes bear direct information concerning the absorption spectra of these structures.

Figure 2 shows spectral dependences of the photostimulated formation of O^- radical anions upon the irradiation of oxide semiconductors (TiO_2 [3, 35] and ZnO [4]) and dielectrics (MgO [10, 12] and CaO [11, 12]). It was demonstrated in the cited studies that these photostimulated processes include primary light absorption by coordinatively unsaturated surface structures and, in all cases, can be described by the following scheme:

$$(Me^{n+}–O^{2-})_{LC} \underset{}{\overset{h\nu}{\rightleftharpoons}} (Me^{(n-1)+}–O^-)^*_{LC} \qquad \text{(VIII.1)}$$

$$(Me^{(n-1)+}–O^-)^*_{LC} \xrightarrow{+RH} (Me^{(n-1)+}–OH^-)_{LC} + R^\bullet \qquad \text{(VIII.2)}$$

$$(Me^{(n-1)+}–O^-)^*_{LC} \xrightarrow{+O_2} O_2^- + [O^-_{LC}...O_2] \qquad \text{(VIII.3)}$$

$$(Me^{(n-1)+}–O^-)^*_{LC} \rightarrow [e]_{st} + (O^-_{LC})_{st} \qquad \text{(VIII.4)}$$

$$(Me^{(n-1)+}–O^-)^*_{LC} \xrightarrow{+N_2O} (O^-)_{ads} + (O^-_{LC})_{st} \qquad \text{(VIII.5)}$$

(st = stabilized species).

Reaction (VIII.2) involves oxidizable RH molecules from the gas phase and results in the photoreduction of the cation. As was mentioned above, this is a typical reaction of the short-lived radical anion O^- of the triplet excited complex $(Me^{(n-1)+}–O^-)^*_{LC}$.

The absorption bands of this complex vary, depending on the surface structure to which the complex is bound. Owing to this fact, use of monochromatic light makes it possible in some cases to selectively generate O^-_{LC}, radical anions with different coor-

Table 1. Comparative characteristics of the efficiency of formation of oxygen radical anions resulting from irradiation of oxides in the spectral region of their surface absorption

Characteristic	TiO_2 [3, 35]	SnO_2 [37]	MgO [10, 12, 36]	CaO [11, 12, 36]	ZnO [4]
"Memory" effect* in the formation of O^- and O_2^- radical anions, %	<1	<1	~3	~50	>90
O_2 pressure starting at which the efficiency of formation of radical anions stop increasing, Torr	~100	~1	$\sim10^{-3}$	–	$<10^{-6}$
Estimated lifetime of the excited state, s	$\sim10^{-8}$	$\sim10^{-6}$	$\sim10^{-3}$	–	$>10^3$

* In the determination of the memory effect, irradiation was performed in vacuo and oxygen was adsorbed after the irradiation was finished. The memory effect was determined as the ratio of the concentration of the radical anions obtained via this procedure to their concentration attained by irradiation in oxygen for the same time.

dination spheres [11, 12, 36]. Reactions (VIII.3)–(VIII.5) take place in all systems examined. The oxides differ significantly in spectral characteristics of photostimulated processes (Fig. 2), in the stability of the resulting radical anions, and in the efficiency of formation of these species.

Note that the efficiency of formation of electron centers and holes is low for most oxides irradiated in vacuo (Table 1). However, the introduction of the electron acceptor O_2 (reaction (VIII.3)) or N_2O (reaction (VIII.5)) into the gas phase can raise the efficiency of this process by a factor of several tens (MgO) or several hundreds (TiO_2, SnO_2).

The efficiency of formation of oxygen radical anions under irradiation of the surface in the presence of O_2 stops increasing once a certain critical pressure is reached. This pressure varies significantly from one system to another (Table 1). It is likely that, at pressures above the critical value, the frequency of collisions of O_2 molecules with adsorption sites (excited $[Me^{(n-1)+}...O^-]$* complexes) does not limit the rate of this process. Hence, under the assumption that reaction (VIII.3) proceeds via the Eley–Rideal mechanism and this reaction occurs with a probability of about 1 upon collision between an O_2 molecule and an adsorption site, it is possible to estimate the minimum lifetime of the excited complex (Table 1). The lifetime of the excited state for MgO was thus estimated at $\sim10^{-3}$ s, which is in good agreement with the data obtained for this system by chemiluminescent methods [25].

Now we will discuss our results concerning the photostimulated processes in oxide dielectrics (MgO and CaO) and semiconductors (ZnO) in greater detail.

MgO. Figure 3 (curve *2*) shows a typical EPR spectrum obtained upon the irradiation ($h\nu = 4.43$ eV) of MgO in vacuo at 298 K. Along with signals from bulk centers ($g_{av} = 2.01, g_{av} = 2.004$) and Mn^{2+} cations, there are weak lines from the surface radical anion $(O^-)_{st}$ with $g_\perp^1 = 2.042$ and $g_\perp^2 = 2.032$. Stabilized surface electron centers (F^+ centers) cannot be observed under these conditions because of their short lifetime at 298 K. Note the low efficiency of the formation of surface paramagnetic centers in the irradiation of MgO in vacuo at 298 K (reaction (VIII.4)). Also low are their limiting concentrations attainable by prolonged irradiation.

The irradiation of the same MgO sample at 298 K in the presence of electron acceptor molecules of O_2 raises the concentration of surface-stabilized electron and hole centers by a factor of 30–50, as in the case of titanium dioxide [3, 35] and tin dioxide [37]. When O_2 is present in the gas phase, the hole centers show themselves as $[O^-...O_2]$ complexes, which turn reversibly into $(O^-)_{st}$ radical anions upon pumping at 298 K (Fig. 3, curves *1*, *1*a). The electron centers manifest themselves as the radical anion O_2^-.

The EPR spectra presented in Fig. 3 clearly show that there are different O^- radical anions on the MgO surface, as is indicated by the somewhat different $g_\perp$ values ($g_\perp^1 = 2.042$; $g_\perp^2 = 2.032$; $g_\perp^3 = 2.044$). These radicals differ in their thermal stability [38] and in the heat of formation of the molecular complex $[O^-...O_2]$ resulting from their interaction with oxygen (Fig. 3a). Their common features are that all of them are stable at 298 K, are observable by EPR, and, interacting with O_2, yield the molecular complex $[O^-...O_2]$ with the following EPR parameters: $g_1 = 2.017$, $g_2 = 2.010$, and $g_3 = 2.002$ ($T = 100$ K) [12, 36, 39]. Based on the results of those studies, these radicals can be identified as tricoordinated O^- radicals (hereafter, O_{3C}^-). The difference between the $g_\perp$ values for these radicals is due to the difference between their locations and was also

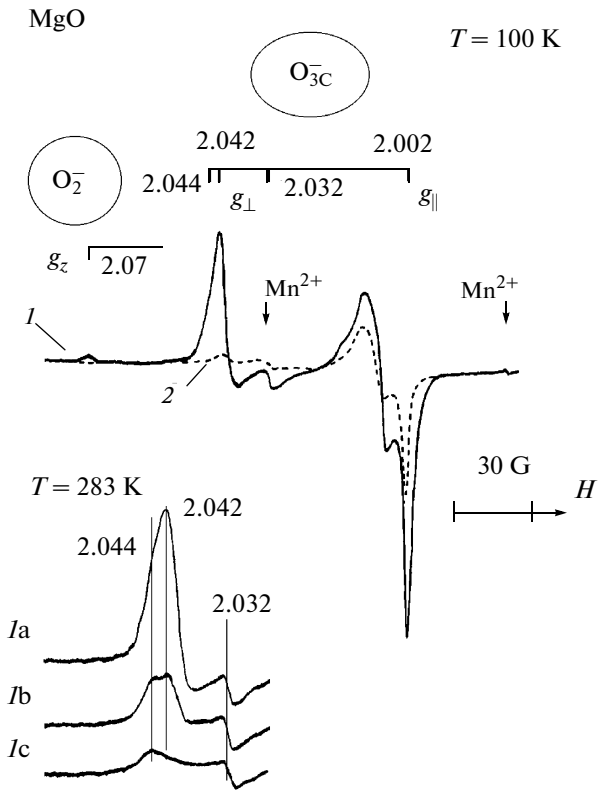

Fig. 3. EPR spectra observed after the irradiation of MgO (*1*) at an oxygen pressure of 66 Pa and (*2*) in vacuo ($h\nu = 4.43$ eV, $t = 90$ min, $T = 298$ K). Spectrum *1* was recorded after the sample was pumped at 298 K. The spectra were obtained at 100 K. Fig. 3a: EPR spectra obtained in the same way as spectrum *1* (*1*a) in vacuum and at equilibrium O_2 pressures of (*1*b) 1.2×10^{-2} and (*1*c) 9.3×10^{-3} Pa; the spectra were recorded at 283 K.

observed by other authors [31, 33]. Accordingly, the complex between O^-_{3C} and dioxygen will be designated $[O^-_{3C}...O_2]$.

Markedly different properties are shown by O^- radical anions hypothetically bound to tetracoordinated structures (hereafter, O^-_{4C}), discovered in our earlier works [12, 36, 39]. They are thermally much less stable and disappear almost entirely via recombination at $T > 250$ K. At the same time, attempts to directly observe their EPR spectra have failed. An appropriate spin probe for their detection and study is their complexes with dioxygen, $[O^-_{4C}...O_2]$ (Table 2, Fig. 4), with EPR parameters of $g_1 = 2.015$, $g_2 = 2.010$, and $g_3 = 2.002$ [39]. It is these radical anions that are dominant under low-temperature irradiation of the sample with monochromatic light ($\lambda = 303$ nm) at short exposure times (Fig. 4, curve *1*). Extending the exposure time leads to an increase in the concentration of these species, to the appearance of $[O^-_{3C}...O_2]$ complexes, and to an increase in their contribution to the overall spectrum. Figure 4 (curve *2*) shows a typical spectrum characterizing the limiting concentration of the radical anions generated by prolonged irradiation. Clearly, the contribution from the complexes $[O^-_{3C}...O_2]$ and $[O^-_{4C}...O_2]$ to the overall spectrum *2* are similar.

The heat of formation of $[O^-_{4C}...O_2]$ is much lower than that of $[O^-_{3C}...O_2]$. Because of this, short-term pumping at 180–200 K causes the reversible disappearance of the former (Fig. 4, curve *3*) as a result of the shift of the $[O^-_{4C}...O_2] \Leftrightarrow [O^-_{4C} + O_2]$ equilibrium to the right. As this takes place, the O^-_{4C} centers persist, and subsequent oxygen adsorption reproduces spectrum *2* (Fig. 4). This pumping does not change the $[O^-_{3C}...O_2]$ concentration. It is, therefore, possible to prepare a sample containing bound O^-_{3C} radical anions ($[O^-_{3C}...O_2]$ complexes) and free O^-_{4C} radical anions. Figure 5 illustrates the results of the interaction of this sample with ^{13}CO molecules at 163 K. The EPR spectrum clearly indicates the appearance of components

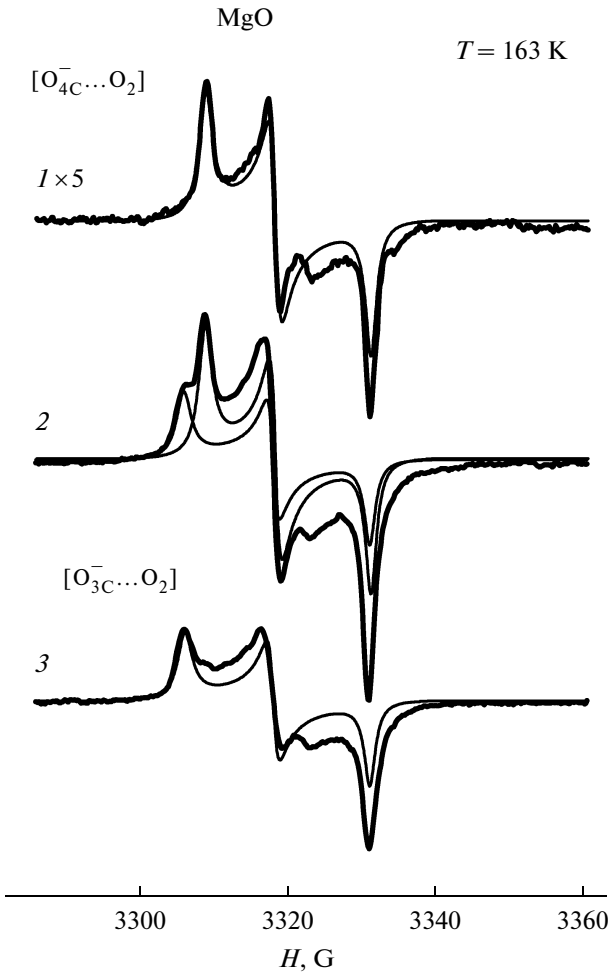

Fig. 4. EPR spectra observed after the irradiation ($h\nu$ = 4.09 eV) of MgO at 163 K and an oxygen pressure of 0.04 Torr for (*1*) 1 min, (*2*) 40 min, and (*3*) after subsequent 20-min-long pumping of the sample at 303 K. The spectra were recorded at 163 K. The thin lines show the simulated EPR spectra with $g_1 = 2.0155$, $g_2 = 2.010$, and $g_3 = 2.002$ (spectrum *1*) and with $g_1 = 2.0175$, $g_2 = 12.010$, and $g_3 = 2.002$ (spectrum *2*), which are close to the parameters listed in Table 1.

characteristic of the radical anion $^{13}CO_2^-$ [40–42], which results from the reaction

$$\left[Mg^{2+}...O^-\right](S=1/2) + CO \rightarrow \left[Mg^{2+}...CO_2^-\right](S=1/2). \quad \text{(IX)}$$

Note that, at 163 K, the free O_{4C}^- radical anion reacts readily with other oxidizable molecules (H_2, CH_4, C_2H_4), while the $[O_{3C}^-...O_2]$ complex does not.

CaO. On the whole, the mechanism of the photostimulated formation of oxygen radical anions on the

Table 2. EPR parameters of various types of O^- radical anions and $[O^-...O_2]$ complexes on the surface of different oxides

Oxide	O_{3C}^-		$[O_{3C}^-...O_2]$			O_{4C}^-	$[O_{4C}^-...O_2]$			Reference
	$g_\perp$	$g_\parallel$	g_1	g_2	g_3		g_1	g_2	g_3	
MgO	2.033–2.044 for $T > 250$ K	2.002	2.017	2.010	2.002	Unobs.*	2.015	2.010	2.002	[10, 12, 36]
			$g_\perp = 2.013$		$g_\parallel = 2.002$					
CaO	Unobs.*		2.015	2.009	2.002	Unobs.*	$g_\perp = 2.012$		$g_\parallel = 2.004$	[11, 12, 36]
			2.016	2.009	2.002					
ZnO	2.021	2.003	$g_\perp = 2.003$		$g_\parallel = 2.008$					[4]
	2.023	2.003								
TiO_2	Unobs.*		$g_\perp = 2.001$		$g_\parallel = 2.008$					[3, 35]

* Unobs. = radical anion unobservable by EPR.

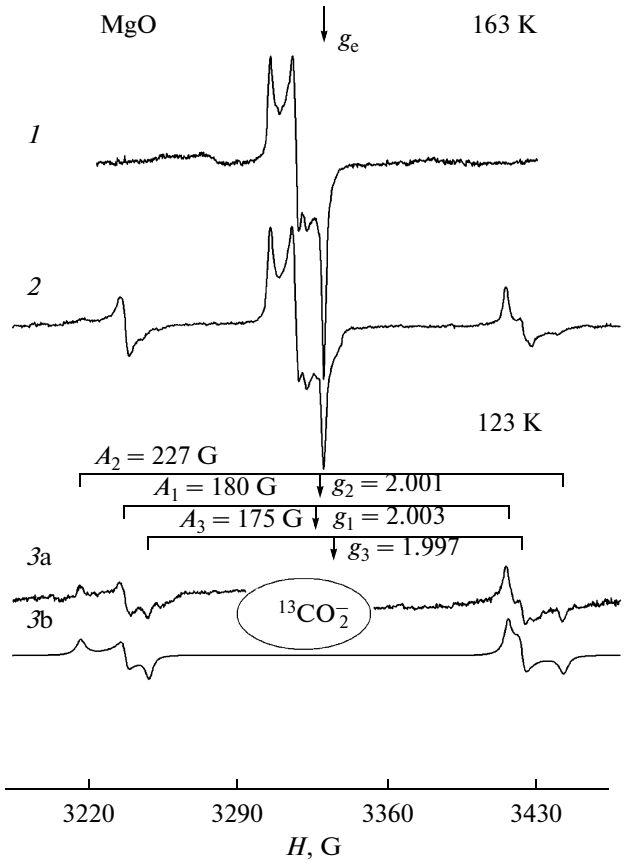

Fig. 5. EPR spectra observed after the interaction of MgO with ^{13}CO: (*1*) spectrum obtained in the same way as spectrum *3* in Fig. 4); (*2*, *3*a) spectra obtained after additional adsorption of ^{13}CO (^{13}C isotope enrichment of 60%) at 0.02 Torr and 163 K; (*3*b) simulated spectrum of the CO_2^- radical anion with $g_1 = 2.003$, $g_2 = 2.001$, and $g_3 = 1.997$; $A_1(^{13}C) = 180$ G, $A_2(^{13}C) = 227$ G, $A_3(^{13}C) = 175$ G. The spectra were recorded at (*1*, *2*) 163 and (*3*a) 123 K.

CaO surface is similar to the mechanism considered above for MgO. For this reason, we will point out only the most significant distinctions between these systems: (1) The spectral dependences of these photostimulated processes in CaO are red-shifted relative to the same dependences for MgO (Fig. 2), which is due to the narrower band gap of CaO. (2) The preirradiation memory effect is close to 50% for CaO and does not exceed 3% for MgO (Table 1). This means that the irradiation of CaO in vacuo causes very efficient O_{3C}^- and O_{4C}^- formation. (3) In the case of CaO, it is impossible to observe the EPR spectra of O_{3C}^- and O_{4C}^-. Therefore, test reactions have to be used in their detection [11, 12, 36, 43]. A convenient test for their detection and concentration measurement is their interaction with dioxygen, which yields the surface molecular complexes $[O_{3C}^-...O_2]$ and $[O_{4C}^-...O_2]$, as in the case of MgO.

Figure 6 shows the EPR spectrum of the initial CaO sample pumped at 773 K (curve *1*) and the spectrum of the same sample subjected to prolonged irradiation with monochromatic light ($\lambda = 313$ nm) in vacuo at 123 K (curve *2*). A weak signal with $g < g_e$ ($g = 1.998$) can clearly be seen, which is due to the appearance of stabilized electron centers. No EPR lines due to the appearance of O^- hole centers are observed. However, subsequent exposure of the sample to O_2 at 123 K gives rise to an intense EPR signal (curve *3*) due to the molecular complexes $[O_{3C}^-...O_2]$ ($g_1 = 2.0164$, $g_2 = 2.0095$, $g_3 = 2.0026$) and $[O_{4C}^-...O_2]$ ($g_\perp = 2.0126$, $g_\parallel = 2.0044$). Irradiation of the sample in an oxygen atmosphere raises the concentration of these radicals by a factor of 2–2.5 (curve *4*), which is consistent with the above-mentioned memory effect of about 50% (Table 1). Figure 7 presents the experimental (curve *1*) and simulated (curves a, b, a + b)

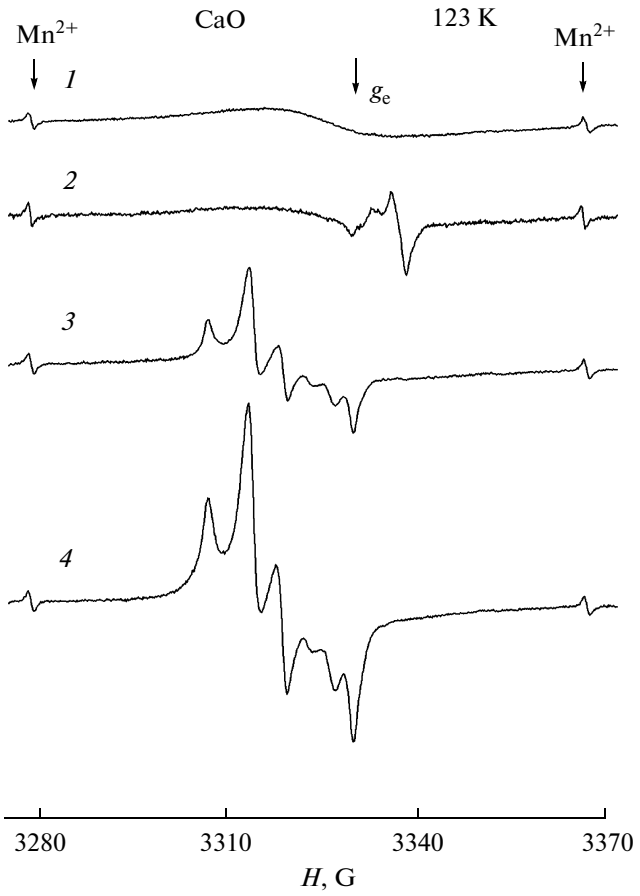

Fig. 6. EPR spectra of the initial oxidized CaO sample recorded (*1*) in vacuo, (*2*) after irradiation with $\lambda = 303$ nm light in vacuo for 40 min, (*3*) after subsequent O_2 adsorption (0.03 Torr), and (*4*) after additional irradiation with $\lambda = 303$ nm light at the same oxygen pressure. The sample was treated at 123 K in all cases, and the spectra were recorded at the same temperature.

spectra of the $[O^-...O_2]$ complex characterized by the above EPR parameters.

As in the case of MgO, for CaO the heat of formation of the $[O^-_{4C}...O_2]$ complex is substantially lower than that of the $[O^-_{3C}...O_2]$ complex. Short-term pumping at 160–180 K causes the reversible disappearance of the $[O^-_{4C}$ ... $O_2]$ complex, while the $[O^-_{3C}...O_2]$ complex is stable under these conditions. Thus, for CaO it is also possible to prepare a sample containing bound O^-_{3C} radical anions ($[O^-_{3C}...O_2]$ complexes) and free O^-_{4C} radical anions.

ZnO. The mechanism of the photostimulated formation of oxygen radical anions on the ZnO surface is similar to the mechanism considered above for MgO and CaO. However, note the following most significant distinctions between these systems: (1) The spectral dependence of these photostimulated processes in ZnO is shifted to the visible region (Fig. 2), which is due to ZnO having a much narrower band gap than MgO or CaO. (2) The preirradiation memory effect for ZnO is close to 100%. This means that the appearance of oxygen or N_2O in the gas phase exerts almost no effect on the efficiency of radical anion formation. (3) ZnO is the only presently known system in which irradiation generates pairs of hole sites (O^- radical anions) and electron centers (Zn^+ ions) [4].

As in the above systems, the O^- radical anions and Zn^+ ions are spatially separated and react independently with molecules of the gas phase. For example, only O^- reacts with oxidizable molecules of CO and CH_4:

$$\left[Zn^{2+}...O^-\right](S = 1/2) + CO \rightarrow \left[Zn^{2+}...CO_2^-\right](S = 1/2), \quad \text{(X)}$$

$$\left[Zn^{2+}...O^-\right](S = 1/2) + CH_4 \rightarrow \left[Zn^{2+}...OH^-\right](S = 0) + {}^{\bullet}CH_3(S = 1/2). \quad \text{(XI)}$$

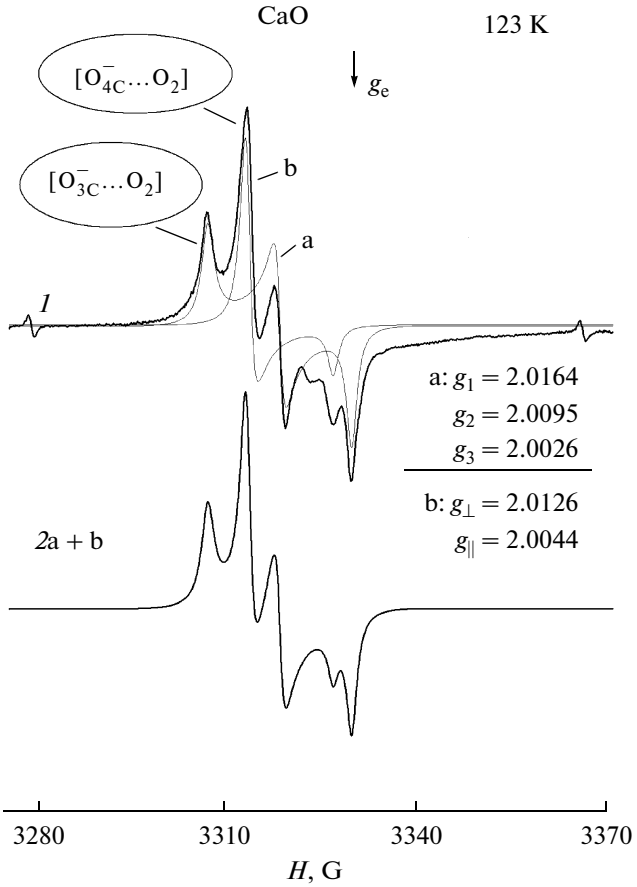

Fig. 7. EPR spectra of $[O^-...O_2]$ complexes on CaO: (*1*) the same as spectrum *4* in Fig. 6; (a, b) simulated spectra, with parameters indicated on the figure panel; (*2*) sum of the spectra (a) and (b).

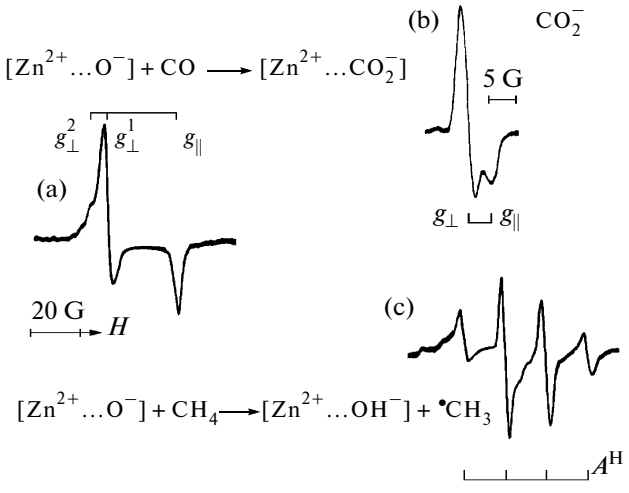

Fig. 8. (a) EPR spectrum of photoinduced O^- radical anions on the ZnO surface and (b, c) those of the radicals resulting from the interaction of ZnO with (b) CO and (c) CH_4. The spectra were recorded at (a, c) 90 and (b) 160 K.

The Zn^+ ion does not react with these molecules [41, 44]. Figure 8 shows the EPR spectra of the radicals resulting from these reactions. Note that the reaction between $[Zn^{2+}...O^-]$ and CO is not accompanied by a change in the spin of the initial complex: the $[Zn^{2+}...CO_2^-]$ radical anion also has a spin of $S = 1/2$ and is detectable by EPR in a rather wide temperature range. At the same time, the reaction of the zinc complex with methane (and other hydrogen-containing molecules) is typically accompanied by a change in the spin, yielding the paramagnetic complex $[Zn^{2+}...OH^-]$. The $^\bullet CH_3$ radical that has escaped from the reaction "cage" is stable on the ZnO surface only at low temperature of $T < 90$ K [44] and is detectable by EPR (Fig. 8, curve c). Note that the escape of $^\bullet CH_3$ radicals into the gas phase as a result of similar reactions on the MgO and Li/MgO surfaces was observed by other authors [45–47].

Thus, the above data demonstrate that, in all cases, the O^- radical anions are stabilized on diamagnetic ions. Owing to this circumstance, either these radical anions themselves or the radical anions resulting from their reaction with O_2 (reactions (VIII.3) and (VIII.4)) or CO (reactions (IX) and (X)) are detectable by EPR. This is due to the fact that all of these species have a half-integer spin ($S = 1/2$) and this spin is unaffected by the occurring reaction. At the same time, the interaction of these species with hydrogen-containing molecules typically changes the spin (reaction (XI)), yielding a diamagnetic product.

α-Oxygen in Zeolite FeZSM-5 and Its Reactions

So-called α-oxygen [6, 48, 49] (O_α), which is responsible for the selective oxidation of organic compounds by N_2O over zeolite FeZSM-5, is the only presently known example of an O^- radical anion stabilized on a paramagnetic ion. According to the literature [6, 48–50], the mechanism of its formation can be described by the following scheme:

$$\left[Fe^{2+}\right](S=2) + N_2O \rightarrow \left[Fe^{3+}...O^-\right](S=2) + N_2. \quad \text{(XII)}$$

The radical difference between this scheme and schemes (III), (IIIa), and (VIII.5) is the integer spin ($S = 2$) of the initial electron-excessive complex $[Fe^{2+}]$ and, accordingly, the integer total spin of the complex $[Fe^{3+}...O^-]$—radical anion O^- stabilized on a paramagnetic ion. This is the reason why neither $[Fe^{2+}]$ nor $[Fe^{3+}...O^-]$ can be directly detected by EPR.

In order to investigate such systems, we earlier suggested a spin design technique, specifically, purpose-oriented change of the spin state of a complex by reacting it with molecules of the gas phase so that the resulting complex has a half-integer spin and is readily detectable by EPR [50–53]. This approach proved

very informative in the study of $[Fe^{2+}]$ complexes [50, 52] using the reaction

$$\left[Fe^{2+}\right](S = 2) + NO \rightarrow \left[Fe^{3+}...NO^{-}\right](S = 3/2) \quad \text{(XIII)}$$

as well as in the investigation of the reactions of $[Fe^{3+}...O^{-}]$ (α-oxygen) with hydrogen and methane [50, 53]. It was demonstrated that these reactions yield the same paramagnetic complex $[Fe^{3+}...OH^{-}]$ with $S = 5/2$:

$$\left[Fe^{3+}...O^{-}\right](S = 2) + H_2, \quad CH_4 \rightarrow \left[Fe^{3+}...OH^{-}\right](S = 5/2). \quad \text{(XIV)}$$

The formation of complexes with $S = 5/2$ (signal with $g = 4.3$) is also observed in the interaction between α-oxygen and an NO molecule (Fig. 9, curve *1*):

$$\left[Fe^{3+}...O^{-}\right](S = 2) + NO \rightarrow \left[Fe^{3+}...NO_2^{-}\right](S = 5/2). \quad \text{(XV)}$$

It is clear from the data presented in Fig. 9 that NO adsorption gives rise both to signals from the $[Fe^{3+}...NO_2^{-}]$ ($S = 5/2$) complexes and to a signal near g_e ($g_\perp = 1.99$, $g_\parallel = 1.86$) from weakly bound $[NO...A_S]$ complexes, which are due to the stabilization of the NO molecule on nonparamagnetic Lewis acid sites (A_S) of the zeolite [54, 55]:

$$[A_S](S = 0) + NO \rightarrow [A_S...NO](S = 1/2). \quad \text{(XVI)}$$

Subsequent exposure of the sample to oxygen at 123 K causes the oxidation of adsorbed NO to NO_2, giving rise to the EPR spectrum characteristic of this radical [56, 57] (Fig. 9, curve *2*):

$$[A_S...NO](S = 1/2) + O_2 \rightarrow \left[A_S...NO_3^{-}\right](S = 1/2). \quad \text{(XVII)}$$

This is not accompanied by any change in the spectra of the $[Fe^{3+}...NO_2^{-}]$ complexes.

We were unable to detect the appearance of any paramagnetic complexes in the interaction of α-oxygen with CO and O_2 molecules. These reactions for "ordinary" O^- radical anions take place without a change in the spin: the resulting CO_2^- radicals and $[O^-...O_2]$ complexes have a spin of $S = 1/2$, like the primary O^- radicals. It can be assumed that, for α-oxygen, these reactions proceed according to the similar schemes

$$\left[Fe^{3+}...O^{-}\right](S = 2) + CO \rightarrow \left[Fe^{3+}...CO_2^{-}\right](S = 2), \quad \text{(XVIII)}$$

$$\left[Fe^{3+}...O^{-}\right](S = 2) + O_2 \rightarrow \left[Fe^{3+}...O^{-}...O_2\right](S = 2). \quad \text{(XIX)}$$

without changing the spin of the initial complex ($S = 2$). Only in this case will the paramagnetic complexes have an integer spin and be directly unobservable by EPR.

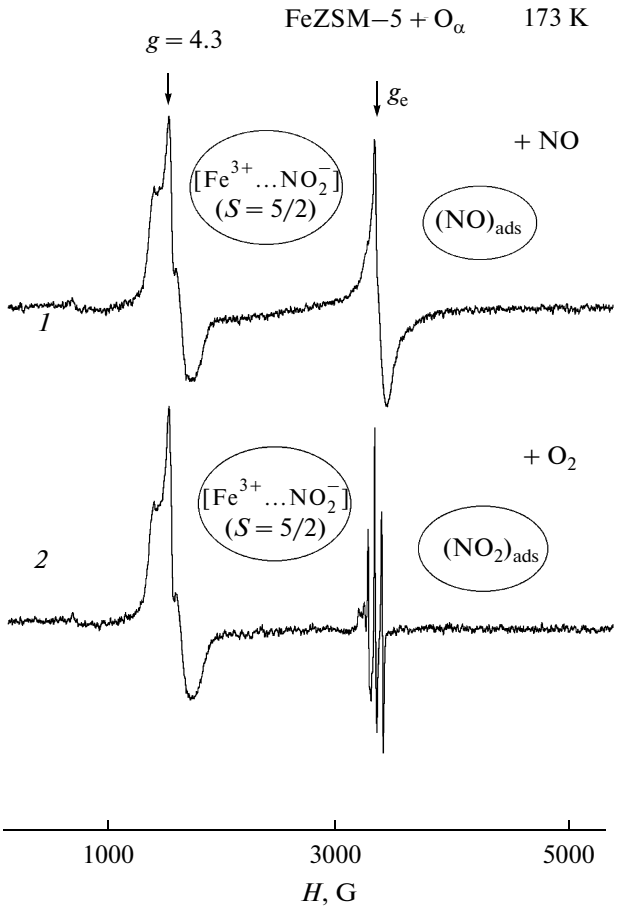

Fig. 9. EPR spectra observed (*1*) after NO adsorption at 173 K on zeolite FeZSM-5 containing adsorbed α-oxygen and (*2*) after additional exposure of the sample to oxygen (0.1 Torr) followed by pumping at 173 K. The spectra were recorded at 173 K.

Thus, the EPR data indicate that, in all of its known reactions (Table 3), α-oxygen behaves in the same way as "ordinary" O^- radical anions. The only difference between these species is in their spin: $S = 2$ for α-oxygen and $S = 1/2$ for O^- stabilized on diamagnetic cations. It is, therefore, natural that, in the reactions in which the spin state remains unchanged (reactions of these species with CO and O_2), paramagnetic products with a half-integer spin ($S = 1/2$) are observed only for the O^- radical anions, while in the react ions changing the spin state (reactions with H_2, CH_4, and NO), paramagnetic products with $S = 1/2$ are observed only for α-oxygen.

A special place among the above reactions of the O^- radical anions (Table 3) is occupied by the interaction of these species with ethylene. Depending on the properties of their stabilization sites, this reaction may result in the addition of ethylene, yielding the paramagnetic product $C_2H_4O^-$ ($S = 1/2$) [58–60], or in the

Table 3. Reactions of O^- radical anions on oxide surfaces and those of α-oxygen on zeolite FeZSM-5 (EPR-detectable paramagnetic species are bold-typed)

Entry	Reactant	Radical anion O^-: **$[Me^{n+}–O^-]$, S = 1/2;** $Me^{n+} = Mg^{2+}, Ca^{2+}, Zn^{2+}, V^{5+}, Mo^{6+}, W^{6+}, ...$	α-Oxygen: $[Fe^{3+}–O^-]$, S = 2;
1	$+H_2$	$\longrightarrow [Me^{n+}–OH^-]$, S = 0 + **$(H^\bullet)$, S = 1/2**	$\longrightarrow$ **$[Fe^{3+}–OH^-]$, S = 5/2** + $(H^\bullet)$, S = 1/2
2	$+CH_4$	$\longrightarrow [Me^{n+}–OH^-]$, S = 0 + **$(^\bullet CH_3)$, S = 1/2**	$\longrightarrow$ **$[Fe^{3+}–OH^-]$, S = 5/2** + $(^\bullet CH_3)$, S = 1/2
3	+NO	$\longrightarrow [Me^{n+}–(NO_2^-)]$, S = 0 **(?)**	$\longrightarrow$ **$[Fe^{3+}–NO_2^-]$, S = 5/2**
4	+CO	$\longrightarrow$ **$[Me^{n+}–(CO_2^-)]$, S = 1/2;**	$\longrightarrow [Fe^{3+}–CO_2^-]$, S = 2 **(?)**
5	$+O_2$	$\longrightarrow$ **$[Me^{n+}–(O^-...O_2)]$, S = 1/2;**	$\longrightarrow [Fe^{3+}–(O^-...O_2)]$, S = 2 **(?)**
6	$+C_2H_4$	$\nearrow [Me^{n+}–OH^-]$, S = 0 + **$(^\bullet C_2H_3)$, S = 1/2** $\longrightarrow$ **$[Me^{n+}–(C_2H_4O^-)]$, S = 1/2;** $\searrow [Me^{n+}–OH^-]$, S = 0 + **$(^\bullet R–CH_2)$, S = 1/2**	**(?)**

Note: The EPR-detectable paramagnetic species are bold-typed.

abstraction of a hydrogen atom from the ethylene molecule, yielding the diamagnetic complex $[Me^{n+}...OH^-]$ and the stabilized radical $R^\bullet$, as in reactions (II) and (XIV) [61–63]. It is interesting that the latter situation is observed both in the interaction of ethylene with O^- radical anions stabilized on the surface of MgO [61] or ZnO [63] and in the interaction of ethylene with short-lived $[V^{4+}...O^-]^*$ radical anions [62]. No data concerning the spin state of the products of the interaction between α-oxygen and ethylene have been reported to date.

Thus, a direct comparison of all known reactions of α-oxygen with reactions of "ordinary" O^- radical anions (Table 3) indicates that these reactions are similar. This result can be considered as convincing spectroscopic evidence that α-oxygen is essentially the $[Fe^{3+}...O^-]$ complex, or an O^- radical anion stabilized on a paramagnetic ion.

CONCLUSIONS

The experimental results presented in this work, including relevant data available from the literature, revealed the general regularities of the reactions involving the O^- radical anions. These regularities allow such reactions to be identified even when the O^- radical anions themselves are undetectable by EPR.

These reactions include the following: (1) various reactions involving short-lived the O^- radical anion of triplet excited surface $[V^{4+}...O^-]^*$ complexes; (2) above-considered reactions of EPR-inactive O_{3C}^- and O_{4C}^- radical anions on the CaO and MgO surface; (3) reactions of the α-oxygen species $[Fe^{3+}...O^-]$, the only known example of an O^- radical anion stabilized on a paramagnetic ion.

The approaches suggested here for analysis of such systems, including the spin design methodology, are usable in the identification of O^- radical anions (both observable and unobservable) and in the investigation of their role in chemical reactions on the surface of oxide catalysts, including systems containing paramagnetic ions of transition elements.

A very important feature of the above photostimulated reactions occurring in the spectral range of the surface absorption of the oxides is that their red boundary shifts to longer wavelengths as the band gap of the oxide narrows. For titanium and zinc oxides, the formation of O^- radical anions and all of their typical reactions are possible under irradiation with visible light.

In all photostimulated reactions, O^- radical anions act as electron-deficient (hole) centers. The role of charge-compensating, electron-excessive (electron) centers can be played by Zn^+ ions in ZnO, Ti^{3+} ions in TiO_2, and $F_s(H)$-centers in MgO and CaO. However, although spatially separated electron and hole centers are detectable by EPR, until recently there was no information reported on the mechanism of their spatial separation. It was conventionally assumed that this process is due to the motion of charged particles, either electrons or holes, on the surface, followed by their stabilization on local surface states.

In our recent study [64], we have carried out an analysis of the mechanism of the photostimulated processes responsible for the formation of spatially separated electron and hole centers on the MgO surface. It

was demonstrated for the first time that these processes can occur owing to the spatial separation of not charged particles, but neutral radicals resulting from the homolytic photodissociation of chemisorbed water. The key element of our approach is taking into account the effect of chemisorbed water on the formation and stabilization of O^- radical anions in photostimulated processes. It was shown that the tricoordinated structures containing chemisorbed water (designated as $[OH^-...Mg^{2+}–O^{2-}...H^+]_{3C}$ complexes) may be responsible both for the primary absorption of light quanta and for the subsequent stabilization of O^- radical anions:

$$\left[OH^-...Mg^{2+}–O^{2-}...H^+\right]_{3C} \xrightarrow{h\nu} \left[OH^-...Mg^{+}–O^{-}...H^+\right]^*_{3C} \rightarrow \left[OH^-...Mg^{2+}–O^-\right]_{3C} + H^\bullet. \quad \text{(XX)}$$

The resulting hole center $[OH^-...Mg^+–O^-]_{3C}$ is electroneutral and possesses all properties of the above described radical anion O^-_{3C}. Formally, the formation of this center can be described as the stabilization of the neutral radical $^\bullet OH$ on the coordinatively unsaturated structure $[Mg^{2+}–O^{2-}]_{3C}$:

$$^\bullet OH + \left[Mg^{2+}–O^{2-}\right]_{3C} \rightarrow \left[OH^-...Mg^{2+}–O^-\right]_{3C}. \quad \text{(XXI)}$$

The formation of electron centers through the interaction of $[Mg^{2+}–O^{2-}]_{3C}$ with the neutral radical $H^\bullet$ takes place via a similar mechanism:

$$H^\bullet + \left[Mg^{2+}–O^{2-}\right]_{3C} \rightarrow \left[Mg^{+}–O^{2-}...H^+\right]_{3C}. \quad \text{(XXII)}$$

Our approach easily resolves the paradox of the existence of "electron" O^- radical anions (resulting from reactions (III) and (VIII.5)) and "hole" ones (resulting from reaction (VIII.4)) with identical chemical properties and spectroscopic characteristics on the MgO surface [12, 31]. "Hole" O^- species result in a natural way from reaction (XX) or (XXI); "electron" O^{2-} species, from the interaction of an $F_S(H) = [Mg^+–O^{2-}...H^+]_{3C}$ center with an N_2O molecule:

$$[Mg^+–O^{2-}...H^+]_{3C} + N_2O \rightarrow [OH^-...Mg^{2+}–O^-]_{3C} + N_2. \quad \text{(XXIII)}$$

The final structure of the resulting complexes is the same in both cases.

In the framework of the approach being developed, it can be assumed that the "hole" and "electron" characters of the EPR-detectable O^- radical anions and $F_S(H)$ centers is due not to spatial charge separation, but to electron density redistribution in surface $[Mg^{2+}–O^{2-}]_{3C}$ complexes occurring as a result of reactions (XX)–(XII). The formation of spatially separated paramagnetic centers is due to the transfer of

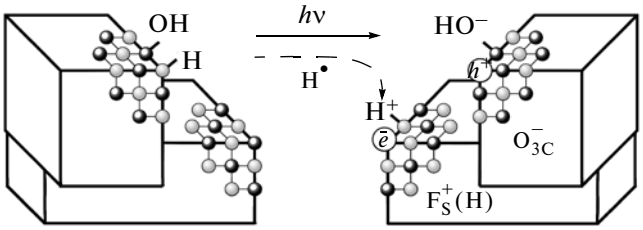

Fig. 10. Formation of electron and hole centers on the MgO surface as a result of the homolytic photodissociation of chemisorbed water.

neutral $H^\bullet$ (or $^\bullet OH$) radicals resulting from the homolytic photodissociation of chemisorbed water (Fig. 10). It is most likely that, because of their electroneutrality, the O^- radical anions (more exactly, $[OH^-...Mg^{2+}–O^-]_{3C}$ complexes) show the properties of a radical, not a hole (electron acceptor), in all of their presently known chemical reactions. This circumstance was pointed out earlier in the literature [12, 65]. Note that impurity bulk hydroxyl groups play a significant role in the formation of radiation-induced V^- centers (O^- radical anions) in MgO single crystals [66]. The magnetic resonance parameters of these centers are similar to those of the surface O^-_{3C} radical anions (Table 2). Note also that the designations O^-_{3C} and O^-_{4C}, used in this work and accepted by other authors for the differently coordinated oxygen radical anions, are a matter of convention and merely conform to the terminology accepted for coordinatively unsaturated structures on the magnesium oxide and calcium oxide surfaces. The actual structure of the surface complexes corresponding to these paramagnetic species is presently unknown and can be determined only by using quantum chemical models describing their experimentally observed magnetic resonance parameters and reactivity.

In conclusion, it should be emphasized that, under all practical experimental conditions, the oxide surface always contains chemisorbed water. The model based on this fact was suggested for the first time in our earlier work [64]. It assumes that O^- radical anions result from the dissociation of chemisorbed water followed by the spatial separation of the radicals. It is based on the partially hydroxylated MgO surface model [67–69], which is presently widespread and can serve as a convenient tool for description of the mechanisms of many thermal and photostimulated processes involving these highly reactive intermediates on oxide surfaces.

ACKNOWLEDGMENTS

This work was supported by the Russian Foundation for Basic Research, grant 10-03-00691a.

REFERENCES

1. Kazanskii, V.B., *Kinet. Katal.*, 1973, vol. 14, no. 1, p. 95.
2. Spiridonov, K.N. and Krylov, O.V., *Probl. Kinet. Katal.*, 1975, vol. 16, p. 7.
3. Cherkashin, A.E., Volodin, A.M., Koshcheev, S.V., and Zakharenko, V.S., *Usp. Foton.*, 1980, vol. 7, p. 86.
4. Volodin, A.M. and Cherkashin, A.E., *Kinet. Katal.*, 1981, vol. 22, no. 3, p. 598.
5. Che, M., Giamello, E., and Tench, A.J., *Colloids Surf.*, 1985, vol. 13, nos. 2–3, p. 231.
6. Panov, G.I., Dubkov, K.A., and Starokon, E.V., *Catal. Today,* 2006, vol. 117, nos. 1–3, p. 148.
7. Lunsford, J.H., *Catal. Rev.*, 1973, vol. 8, no. 1, p. 135.
8. Che, M. and Tench, A.J., *Adv. Catal.*, 1982, vol. 31, p. 77.
9. Che, M. and Tench, A.J., *Adv. Catal.,* 1983, vol. 32, p. 1.
10. Volodin, A.M., *Khim. Fiz.*, 1992, vol. 11, no. 8, p. 1054.
11. Volodin, A.M., Cherkashin, A.E., and Prokop'ev, K.N., *Kinet. Katal.*, 1992, vol. 33, nos. 5–6, p. 1190.
12. Volodin, A.M., *Catal. Today*, 2000, vol. 58, nos. 2–3, p. 103.
13. Volodin, A.M. and Cherkashin, A.E., *React. Kinet. Catal. Lett.*, 1981, vol. 17, nos. 3–4, p. 323.
14. Anpo, M., Che, M., Fubini, B., Garrone, E., Giamello, E., and Paganini, M.C., *Top. Catal.*, 1999, vol. 8, nos. 3–4, p. 189.
15. Bedilo, A.F., Plotnikov, M.A., Mezentseva, N.V., Volodin, A.M., Zhidomirov, G.M., Rybkin, I.M., and Klabunde, K.J., *Phys. Chem. Chem. Phys.*, 2005, vol. 7, no. 16, p. 3059.
16. Il'ichev, A.N., Konin, G.A., Matyshak, V.A., Kulizade, A.M., Korchak, V.N., and Yan, Yu.B., *Kinet. Catal.*, 2002, vol. 43, no. 2, p. 214.
17. Wertz, J.E. and Bolton, J.R., *Electron Spin Resonance: Elementary Theory and Practical Applications*, New York: McGraw-Hill, 1972.
18. Anpo, M., Tanahashi, I., and Kubokawa, Y., *J. Phys. Chem.*, 1980, vol. 84, no. 25, p. 3440.
19. Anpo, M., Tanahashi, I., and Kubokawa, Y., *J. Phys. Chem.*, 1982, vol. 86, no. 1, p. 1.
20. Iwamoto, M., Furukawa, H., Matsukami, K., Takenaka, T., and Kagawa, Sh., *J. Am. Chem. Soc.*, 1983, vol. 105, no. 11, p. 3719.
21. Anpo, M., Higashimoto, S., Matsuoka, M., Zhanpeisov, N., Shioya, Y., Dzwigaj, S, and Che, M., *Catal. Today,* 2003, vol. 78, nos. 1–4, p. 211.
22. Gritskov, A.M., Shvets, V.A., and Kazanskii, V.B., *Kinet. Katal.*, 1974, vol. 15, no. 5, p. 1257.
23. Konnov, A.A., Pershin, A.N., Shelimov, B.N., and Kazanskii, V.B., *Kinet. Katal.*, 1983, vol. 24, no. 1, p. 161.
24. Pershin, A.N., Shelimov, B.N., and Kazanskii, V.B., *Kinet. Katal.*, 1979, vol. 20, no. 5, p. 1298.
25. Anpo, M., Yamada, Y., Kubokawa, Y., Coluccia, S., Zecchina, A., and Che, M., *J. Chem. Soc., Faraday Trans. 1*, 1988, vol. 84, no. 3, p. 751.
26. Shvets, V.A., Vorotinzev, V.M., and Kazansky, V.B., *J. Catal.*, 1969, vol. 15, no. 2, p. 214.
27. Shvets, V.A., Vorotyntsev, V.M., and Kazanskii, V.B., *Kinet. Katal.*, 1969, vol. 10, no. 2, p. 356.
28. Volodin, A.M. and Bol'shov, V.A., *Kinet. Katal.*, 1994, vol. 34, no. 1, p. 127.
29. Launay, H., Loridant, S., Nguyen, D.L., Volodin, A.M., Dubois, J.L., and Millet, J.M.M., *Catal. Today*, 2007, vol. 128, nos. 3–4, p. 176.
30. Chen, K., Bell, A.T., and Iglesia, E., *J. Catal.*, 2002, vol. 209, no. 1, p. 35.
31. Diwald, O., Sterrer, M., Knozinger, E., Sushko, P.V., and Shluger, A.L., *J. Chem. Phys.*, 2002, vol. 116, no. 4, p. 1707.
32. Tench, A.J., Lawson, T., and Kibblewhite, J.F.J., *J. Chem. Soc., Faraday Trans. 1*, 1972, vol. 68, p. 1169.
33. Pinarello, G., Pisani, C., D'Ercole, A., Chiesa, M., Paganini, M.C., Giamello, E., and Diwald, O., *Surf. Sci.*, 2001, vol. 494, no. 1, p. 95.
34. Paganini, M.C., Chiesa, M., Martino, P., Livraghi, S., and Giamello, E., *Stud. Surf. Sci. Catal.*, 2005, vol. 155, p. 441.
35. Volodin, A.M., Cherkashin, A.E., and Zakharenko, V.S., *React. Kinet. Catal. Lett.*, 1979, vol. 11, no. 2, p. 103.
36. Volodin, A.M., Bolshov, V.A., and Konovalova, T.A., *Mol. Eng.*, 1994, vol. 4, nos. 1–3, p. 201.
37. Volodin, A.M., Zakharenko, V.S., and Cherkashin, A.E., *React. Kinet. Catal. Lett*, 1981, vol. 18, nos. 3–4, p. 321.
38. Volodin, A.M., *React. Kinet. Catal. Lett.,* 1984, vol. 25, nos. 3–4, p. 335.
39. Volodin, A.M., *React. Kinet. Catal. Lett.*, 1991, vol. 44, no. 1, p. 171.
40. Meriaudeau, P., Vedrine, J.C., Ben Taarit, Y., and Naccache, C., *J. Chem. Soc., Faraday Trans. 2*, 1975, vol. 71, p. 736.
41. Volodin, A.M. and Cherkashin, A.E., *Kinet. Katal.*, 1981, vol. 22, no. 4, p. 979.
42. Chiesa, M. and Giamello, E., *Chem. Eur. J.*, 2007, vol. 13, no. 4, p. 1261.
43. Volodin, A.M., Cherkashin, A.E., and Prokopiev, K.N., *React. Kinet. Catal. Lett.*, 1992, vol. 46, no. 2, p. 373.
44. Volodin, A.M. and Cherkashin, A.E., *React. Kinet. Catal. Lett.*, 1981, vol. 18, nos. 1–2, p. 243.
45. Driscoll, D.J., Martir, W., Wang, J.X., and Lunsford, J.H., *J. Am. Chem. Soc.*, 1985, vol. 107, no. 1, p. 58.
46. Wang, J.X. and Lunsford, J.H., *J. Phys. Chem.*, 1986, vol. 90, no. 22, p. 5883.
47. Lunsford, J.H., *Langmuir*, 1989, vol. 5, no. 1, p. 12.
48. Dubkov, K.A., Starokon', E.V., Paukshtis, E.A., Volodin, A.M., and Panov, G.I., *Kinet. Catal.,* 2004,vol. 45, no. 2, p. 202.
49. Starokon, E.V., Dubkov, K.A., Pirutko, L.V., and Panov, G.I., *Top. Catal.,* 2003, vol. 23, nos. 1–4, p. 137.
50. Volodin, A.M., Zhidomirov, G.M., Dubkov, K.A., Hensen, E.J.M., and van Santeen, R.A., *Catal. Today*, 2005, vol. 110, nos. 3–4, p. 247.

51. Volodin, A.M., Sobolev, V.I., and Zhidomirov, G.M., *Kinet. Catal.*, 1998, vol. 39, no. 6, p. 775.

52. Volodin, A.M., Dubkov, K.A., and Lund, A., *Chem. Phys. Lett.*, 2001, vol. 333, nos. 1–2, p. 41.

53. Malykhin, S.E., Volodin, A.M., and Zhidomirov, G.M., *Appl. Magn. Reson.*, 2008, vol. 33, nos. 1–2, p. 153.

54. Staudte, B., Gutsze, A., Bohlmann, W., Pfeifer, H., and Pietrewicz, B., *Microporous Mesoporous Mater.,* 2000, vol. 40, nos. 1–3, p. 1.

55. Yahiro, H., Lund, A., and Shiotani, M., *Spectrochim. Acta, Part A*, 2004, vol. 60, no. 6, p. 1267.

56. Lunsford, J.H., *J. Colloid Interface Sci.*, 1968, vol. 26, no. 3, p. 355.

57. Shiotani, M. and Freed, J.H., *J. Phys. Chem.*, 1981, vol. 85, no. 25, p. 3873.

58. Sapozhnikov, V.B., Shvets, V.A., Chuvylkin, N.D., and Kazanskii, V.B., *Kinet. Katal.*, 1976, vol. 17, no. 5, p. 1251.

59. Shvets, V.A., Sapozhnikov, V.B., Chuvylkin, N.D., and Kazansky, V.B., *J. Catal.*, 1978, vol. 52, no. 3, p. 459.

60. Hemidy, J.F. and Tench, A.J., *J. Catal.*, 1981, vol. 68, no. 1, p. 17.

61. Ben Taarit, Y., Symons, M.C.R., and Tench, A.J., *J. Chem. Soc., Faraday Trans.*, 1977, vol. 73, no. 7, p. 1149.

62. Surin, S.A., Shuklov, A.D., Shelimov, B.N., and Kazanskii, V.B., *Khim. Vys. Energ.*, 1977, vol. 11, no. 2, p. 147.

63. Volodin, A.M. and Cherkashin, A.E., *React. Kinet. Catal. Lett.*, 1982, vol. 20, nos. 3–4, p. 347.

64. Malykhin, S.E., Volodin, A.M., Bedilo, A.F., and Zhidomirov, G.M., *J. Phys. Chem. C*, 2009, vol. 113, no. 24, p. 10350.

65. Kazanskii, V.B., *Kinet. Katal.*, 1978, vol. 19, no. 2, p. 279.

66. Chen, Y., Abraham, M.M., Templeton, L.C., and Unruh, W.P., *Phys. Rev. B: Condens. Matter*, 1975, vol. 11, no. 2, p. 881.

67. Murphy, D.M., Farley, R.D., Purnell, I.J., Rowlands, C.C., Yacob, A.R., Paganini, M.C., and Giamello, E., *J. Phys. Chem. B*, 1999, vol. 103, no. 11, p. 1944.

68. Chiesa, M., Paganini, M.C., Giamello, E., Murphy, D.M., Di Valentin, C., and Pacchioni, G., *Acc. Chem. Res.*, 2006, vol. 39, no. 11, p. 861.

69. Napoli, F., Chiesa, M., Giamello, E., Finazzi, E., Di Valentin, C., and Pacchioni, G., *J. Am. Chem. Soc.,* 2007, vol. 129, no. 34, p. 10575.